doi:10.1093/brain/awx131 BRAIN 2017: 140; 2028–2040 | 2028

BRAIN
A JOURNAL OF NEUROLOGY

# Calretinin interneuron density in the caudate nucleus is lower in autism spectrum disorder

**Istvan Adorjan,[1,2] Bashir Ahmed,[1] Virginia Feher,[2] Mario Torso,[3] Kristine Krug,[1] Margaret Esiri,[3] Steven A. Chance[3] and Francis G. Szele[1]**

Autism spectrum disorder is a debilitating condition with possible neurodevelopmental origins but unknown neuroanatomical correlates. Whereas investigators have paid much attention to the cerebral cortex, few studies have detailed the basal ganglia in autism. The caudate nucleus may be involved in the repetitive movements and limbic changes of autism. We used immunohistochemistry for calretinin and neuropeptide Y in 24 age- and gender-matched patients with autism spectrum disorder and control subjects ranging in age from 13 to 69 years. Patients with autism had a 35% lower density of calretinin + interneurons in the caudate that was driven by loss of small calretinin + neurons. This was not caused by altered size of the caudate, as its cross-sectional surface areas were similar between diagnostic groups. Controls exhibited an age-dependent increase in the density of medium and large calretinin + neurons, whereas subjects with autism did not. Diagnostic groups did not differ regarding ionized calcium-binding adapter molecule 1 + immunoreactivity for microglia, suggesting chronic inflammation did not cause the decreased calretinin + density. There was no statistically significant difference in the density of neuropeptide Y + neurons between subjects with autism and controls. The decreased calretinin + density may disrupt the excitation/inhibition balance in the caudate leading to dysfunctional corticostriatal circuits. The description of such changes in autism spectrum disorder may clarify pathomechanisms and thereby help identify targets for drug intervention and novel therapeutic strategies.

1 Department of Physiology, Anatomy and Genetics, University of Oxford, Oxford, UK
2 Department of Anatomy, Histology and Embryology, Semmelweis University, Budapest, Hungary
3 Nuffield Department of Clinical Neuroscience, University of Oxford, Oxford, UK

Correspondence to: Francis Szele, PhD,
Department of Physiology, Anatomy and Genetics,
University of Oxford,
South Parks Road,
Oxford, UK
OX1 3QX
E-mail: Francis.Szele@dpag.ox.ac.uk

Correspondence may also be addressed to: Istvan Adorjan, MD, PhD
Department of Physiology, Anatomy and Genetics,
University of Oxford,
Parks Road,
Oxford, UK
OX1 3QX

**Keywords:** neuroinflammation; microglia; autism spectrum disorder; neuropsychiatry

## Introduction

Autism spectrum disorder has a global prevalence of 0.62% (Elsabbagh *et al.*, 2012) and causes a range of mild to severe motor, interpersonal, cognitive and behavioural manifestations (Geschwind and State, 2015). It probably has a neurodevelopmental aetiology and is associated with several gene mutations and environmental insults such as perinatal inflammation (Depino, 2013; Ebrahimi-Fakhari and Sahin, 2015). There are no effective drugs or behavioural therapies for the disorder and the condition is lifelong with enormous personal and societal burdens (Knapp *et al.*, 2009).

A variety of neuroanatomical and histological abnormalities have been documented, which have been difficult to

Received October 26, 2016. Revised February 20, 2017. Accepted April 18, 2017.

reproduce in animal models. These include enlarged head and brain size (Sacco *et al.*, 2015; Libero *et al.*, 2016). In particular, the cerebral cortex was shown to be increased in size (Hardan *et al.*, 2006; Smith *et al.*, 2016). Several studies have shown that Purkinje cells of the cerebellum are decreased in number in subjects with autism (Kern, 2003; Wegiel *et al.*, 2014*b*).

The vast majority of studies in autism spectrum disorder have focused on altered physiology and histopathology of the cerebral cortex (Fatemi *et al.*, 2002; Gogolla *et al.*, 2009; Oblak *et al.*, 2009, 2011; Morgan *et al.*, 2010; Hashemi *et al.*, 2017). However, there is ample evidence that subcortical structures such as the basal ganglia may underlie some of the behavioural, motor and cognitive symptoms of autism spectrum disorder (Peca *et al.*, 2011; Rothwell *et al.*, 2014; Fuccillo, 2016; Glerean *et al.*, 2016). The caudate nucleus in particular is a nexus of converging circuits including a massive corticostriatal input and therefore it may serve as a node for the pathophysiology of autism spectrum disorder (Kohls *et al.*, 2012; Haber and Behrens, 2014; Fuccillo, 2016).

Interneurons, most of which are inhibitory GABAergic (Cicchetti *et al.*, 2000; Gonchar *et al.*, 2007), have received much attention as being especially relevant for balancing excitation/inhibition in the brain and have been postulated as being disrupted in neuropsychiatric diseases such as schizophrenia (Uhlhaas, 2013; Rogasch *et al.*, 2014) and autism spectrum disorder (Rubenstein and Merzenich, 2003; Coghlan *et al.*, 2012). As distinct subpopulations of GABAergic interneurons, calretinin + and neuropeptide Y + neurons constitute ~15% and ~0.5% of the cortical GABAergic interneurons, respectively (Gonchar and Burkhalter, 1997; Meskenaite, 1997). The proportion of interneurons is greater in the primate than rodent caudate nucleus (Graveland and DiFiglia, 1985) and most of the caudate interneurons are calretinin + (Wu and Parent, 2000). In this study we aimed to compare the density and distribution of the aforementioned interneurons in the caudate nucleus in subjects with autism in order to elucidate the putative striatal excitatory/inhibitory imbalance and contribution to the condition.

# Materials and methods

## Subjects

Subjects were included partly from a former study (autism spectrum disorder $n = 6$, control subjects $n = 6$; Kotagiri *et al.*, 2014) or newly selected from the Oxford Brain Bank (OBB) and the Netherlands Brain Bank (NBB), Netherlands Institute for Neuroscience, Amsterdam (open access: www.brainbank.nl). We studied an age- and gender-matched cohort of 12 subjects with autism spectrum disorder and 12 control subjects. All material was collected from donors from whom written informed consent had been obtained by the OBB or NBB for brain autopsy and use of material and clinical information for research purposes. The demographic characteristics of the cohort are shown in Table 1. The mean values of age, post-mortem interval, time in paraformaldehyde, time in paraffin and processing time (time in paraformaldehyde plus time in paraffin) were similar in both diagnostic groups (Table 1 and Supplementary Table 1).

Sampling was done by the assistants of the OBB and NBB supervised by trained neuropathologists. Depending on availability of tissue blocks from subjects with autism, regions were selected containing the head of the caudate nucleus between 22.5 mm caudal and 13.3 mm rostral to the anterior commissure according to the Human Brain Atlas (Mai *et al.*, 2008) (Supplementary Fig. 1). Corresponding levels of the head of the caudate nucleus were chosen from control subjects. The average position of sampling was similar in both diagnostic groups (Supplementary Tables 1 and 2).

## Immunohistochemistry

Serial sections (6-µm thick) were cut in the coronal plane from paraffin-embedded blocks and mounted on slides. The slides were heated in a thermostat at 76°C for 20 min. Slides were dewaxed and treated with 3% $H_2O_2$ solution (in phosphate-buffered saline, pH 7.4) for 30 min. Antigen retrieval was applied by autoclaving the slides in citrate buffer (0.01 M, pH 6.0) at 121°C for 10 min. The following primary antibodies were used: anti-calretinin (rabbit, 1:300, Chemicon, AB5054), anti-neuropeptide Y (rabbit, 1:250, Abcam, ab30914) and anti-IBA1 (rabbit, 1:500, WAKO, 01919741) in Tris-buffered saline/Triton™ X-100 (pH 7.4) for 1 h. Sections were incubated with horseradish peroxidase-linked secondary antibody from the Envision Kit (Dako, K-5007) for 60 min and labelling was visualized by DAB Substrate Chromogen solution from the same kit, according to manufacturer's protocol. During incubation of primary and secondary antibodies slides were put into a Sequenza System coverplates and rack (Thermo Scientific, 72110017, 73310017). Nuclear counterstain was applied by haematoxylin for 20 s. Slides were dehydrated and coverslipped by DePeX.

## Image analysis, archiving and quantification

Slides were digitized using a slidescanner (Aperio ScanScope AT Turbo, Leica Biosystems) at ×20 magnification and stored on a server (msdlt-slide.dpag.ox.ac.uk). The regions of interest were outlined using the ImageScope programme (Aperio, v11.2.0.780) and the longest diameter of every calretinin + and neuropeptide Y + cell body in the caudate nucleus was manually measured. Two investigators contributed to the calretinin + quantification and both were blinded to the diagnoses of the subjects through random coding of the subject identifiers. In contrast to many other brain diseases where pathology is histologically evident, there were no major histopathological patterns recognizable in the autism cases by our immunohistochemical stainings, and it was not possible to determine—based on any of our immunohistochemistries—which subjects were controls versus autism spectrum disorder. Neuronal cell bodies with a diameter >6 µm and a width >2 µm were included in further statistical analysis (Supplementary Fig. 2). Calretinin + neurons were also counted in the anterior cingulate cortex (Brodmann area 24)

**Table 1 Main demographic characteristics of control and patients with autism spectrum disorder**

| Identifier | Diagnosis | Age | Gender | PMI (h) | Cause of death |
|---|---|---|---|---|---|
| 1105/98 | Control | 13 | M | 72 | Collapse-asystole |
| 137/05 | Control | 16 | M | 72 | Collapse-asystole |
| 1351/93 | Control | 18 | M | 72 | Respiratory failure |
| 3569 | Control | 18 | M | 24 | Subarachnoid haemorrhage |
| 1033/91 | Control | 18 | M | 144 | Vertebral dislocation C5/6 |
| 1134/91 | Control | 21 | F | 24 | Acute cardiac failure |
| 84/07 8B | Control | 26 | F | 10 | Hepatic necrosis |
| 84/07 9B | Control | 40 | M | 40 | Renal failure due to cholangiocarcinoma |
| 52/12 | Control | 42 | F | 48 | Pancreas carcinoma |
| 141/13 | Control | 56 | M | 48 | Cardiovascular collapse |
| 12/71 | Control | 57 | F | 8 | Euthanasia, urothelial carcinoma |
| 149/00 | Control | 69 | F | 96 | Unknown, lung carcinoma |
| 27/12 | ASD | 13 | M | 72 | Suicide |
| 1014/92 | ASD | 17 | M | 72 | CO poisoning |
| 3407 | ASD | 21 | F | n/a | Unknown |
| 84/07 6B | ASD | 21 | M | 48 | Unknown |
| 26/11 | ASD | 22 | M | 48 | SUDEP |
| 07/09 | ASD | 22 | M | 48 | Pulmonary haemorrhage |
| 1158/00 | ASD | 32 | M | 84 | SUDEP |
| 1071/99 | ASD | 33 | F | n/a | Breast carcinoma |
| 84/07 3B | ASD | 42 | M | 46 | Unknown |
| 56/10 | ASD | 44 | F | 72 | Non-Hodgkin lymphoma |
| 162/05 | ASD | 48 | F | n/a | Hyponatraemia |
| 29/12 | ASD | 60 | F | n/a | Gastrointestinal bleeding |

PMI = post-mortem interval; SUDEP = sudden unexplained death in epilepsy.

throughout all layers. It is noted that this part of the anterior cingulate cortex does not have an internal granular layer (layer 4) and has a relatively wide layer 6 (Chana *et al.*, 2003). Occasionally layer 5 pyramidal neurons exhibited a light calretinin staining (in three controls and five autism spectrum disorder subjects) in line with previous observations (Barinka *et al.*, 2010). These neurons were not included in the quantitative analysis. For the IBA1 immunohistochemistry, the stained area fraction was obtained by using the Aperio Positive Pixel Count Algorithm (parameters are shown in Supplementary Table 3). The details of our statistical analyses can be found in the Supplementary material. In brief, Mann-Whitney U-tests, repeated measures ANOVA, univariate ANOVA and Spearman's rank tests were used as appropriate.

# Results

## Morphological assessment of calretinin+ neurons in the caudate nucleus of controls and subjects with autism

We examined the caudate nucleus of 12 control subjects and 12 age and gender-matched patients with autism. Three types of calretinin-immunopositive (calretinin+) neurons were distinguished in the caudate nucleus based on their characteristic morphology and diameter (Fig. 1) (Petryszyn *et al.*, 2014). We qualitatively examined the morphology of 1080 neurons, 180 neurons from each subtype (small, medium, large) in both diagnostic groups (Fig. 1A and B). We next measured the diameters of all calretinin+ neurons present in the caudate nucleus; altogether 17 936 neurons in the control group and 12 677 neurons in the autism spectrum disorder group were counted (Supplementary Fig. 2). The small calretinin+ neurons in controls had round to oval cell bodies, with most being round (Fig. 1I–M). Their diameter ranged from 6 to 15 µm, with an average diameter of $8.67 \pm 0.15$ µm (15 510 neurons measured). The small calretinin+ neurons usually had one or two processes in the plane of the section. The medium-sized neurons in controls had multipolar or bipolar cell bodies (with multipolar dominance) and two to three processes (Fig. 1D and E). Their diameter ranged from 16 to 25 µm with an average diameter of $19.19 \pm 0.16$ µm (1503 neurons measured). The large neurons in controls had multipolar perikarya with three to five processes in the plane of the section (Fig. 1C). Their diameter ranged from 26 to 60 µm with an average diameter of $30.39 \pm 0.34$ µm (923 neurons measured). Qualitative comparison of process numbers, branching and somal shape did not reveal conspicuous morphological differences between the control and autism spectrum disorder groups (Fig. 1F–H and N–R).

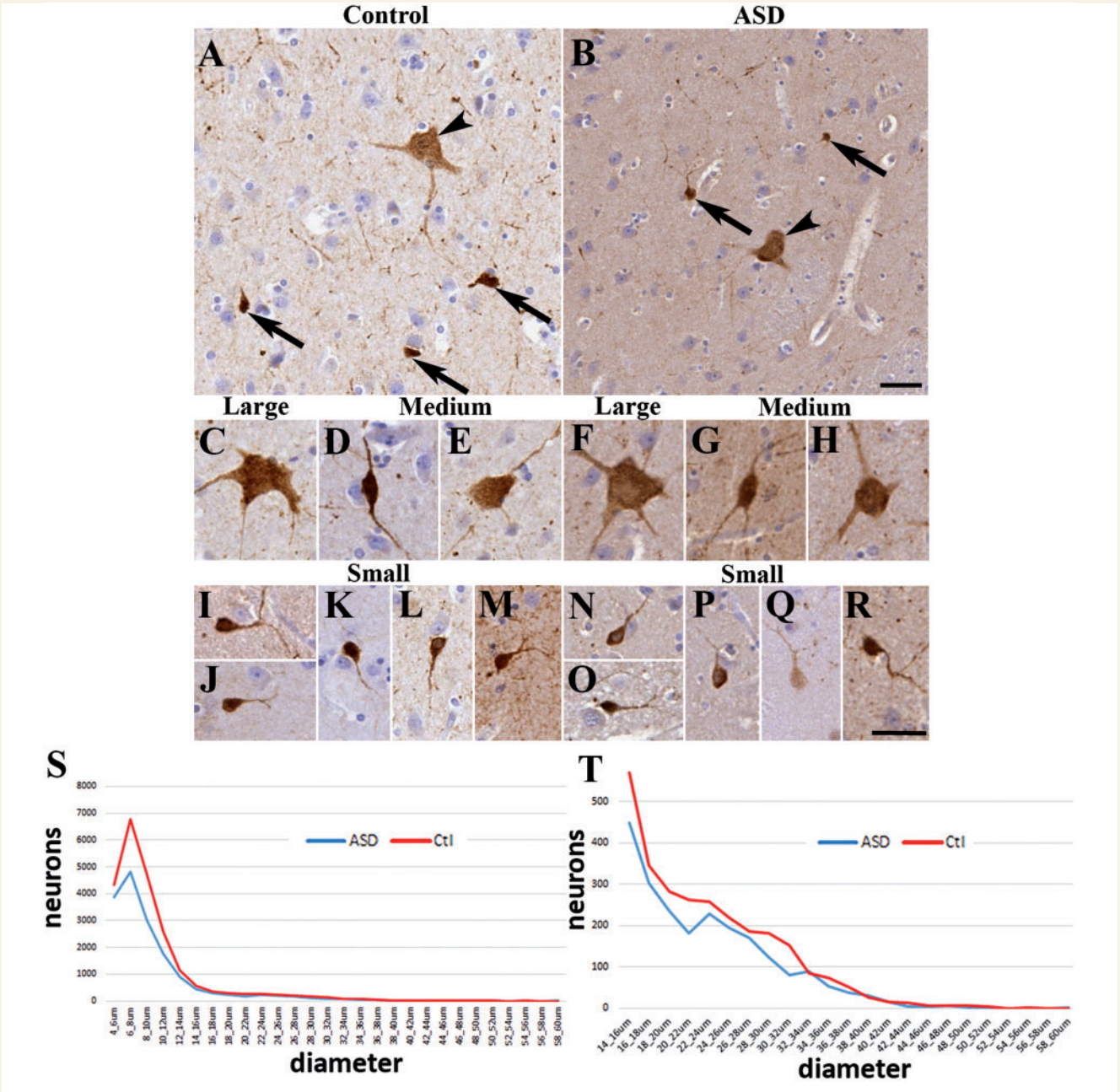


**Figure 1 The morphology of calretinin + neurons in the caudate nucleus was similar in controls and autism spectrum disorder.** Images were taken from four controls and four patients with autism. (**A**) Representative field from controls and (**B**) from autism spectrum disorder (arrowhead, large neuron; arrow, small neuron). (**C**) Large neuron from a control. (**D**) Medium neuron with bipolar morphology from control. (**E**) Medium neuron with multipolar shape from control. (**F**) Large neuron from a subject with autism. (**G–H**) Medium neurons from subjects with autism. (**I–M**) Small neurons from controls. (**N–R**) Small calretinin + neurons from subjects with autism. Scale bars = 30 μm. (**S**) Frequency distribution of calretinin + neurons in the caudate based on the longest diameter measured. Note the characteristic first peak of the calretinin + population (small neurons). (**T**) Frequency distribution of calretinin + neurons in the caudate showing the medium (15–25 μm) and large (>25 μm) populations.

## Diameter and proportion of subgroups of calretinin + neurons in the caudate are unchanged in autism

No significant differences were found between controls and subjects with autism in the average diameters of the calretinin + neurons. Autism spectrum disorder calretinin + neuronal diameters: small 8.66 ± 0.15 μm (10 717 neurons, $P = 0.99$ compared to controls), medium 19.10 ± 0.16 μm (1238 neurons, $P = 0.84$ compared to controls), large 30.41 ± 0.31 μm (722 neurons, $P = 0.97$ compared to controls). The proportions of different calretinin + neuron subtypes (small, medium, large) were also very similar in the groups (controls: 86.47%, 8.39%, 5.14%; autism spectrum

disorder: 84.53%, 9.76%, 5.69%, respectively), in line with a previous report (Wegiel *et al.*, 2014*b*) where neuronal cell body volumes were not changed in the caudate nucleus in subjects with autism ranging from 11 to 60 years old. To confirm the similarities in calretinin + size between controls and subjects with autism we measured the surface area of 40 randomly selected neurons from each case (960 neurons). Similar to the diameter, surface areas were not significantly different between the diagnostic groups: controls: $97.41 \pm 5.89\,\mu m^2$, autism spectrum disorder: $107.34 \pm 5.76\,\mu m^2$, $P = 0.29$. The proportion of the small, medium and large subtypes measured in this analysis were: controls: 87.29%, 8.95%, 3.75%; autism spectrum disorder: 87.5%, 6.79%, 5.7%, respectively. There was a very strong correlation between surface areas and diameters in controls ($r = 0.71$, $P = 7.03 \times 10^{-75}$) and subjects with autism ($r = 0.78$, $P = 3.72 \times 10^{-93}$) that confirmed the validity of diameter measurements and compatibility of the two approaches.

## The density of caudate nucleus calretinin + neurons is lower in subjects with autism

The main finding of this study was a lower density of calretinin + neurons in caudate nucleus in subjects with autism. There was a significant 36.1% decrease in the density of small calretinin + neurons in subjects with autism compared to controls (autism spectrum disorder: $878 \pm 77$ neurons/cm$^2$, controls: $1374 \pm 104$ neurons/cm$^2$, $P < 0.001$) (Fig. 2). Regarding the medium and large subgroups, 25.9% and 27.0% lower densities were seen in the autism group, however these were not statistically significant ($P = 0.242$, $P = 0.590$, respectively, Fig. 2). When the three subgroups were taken together, the autism group showed a statistically significant 34.8% lower density (controls: $1577 \pm 132$ neurons/cm$^2$, autism spectrum disorder: $1028 \pm 97$ neurons/cm$^2$, $P = 0.001$, Fig. 2). There is a paucity of post-mortem human brains from subjects with autism spectrum disorder ($n = \sim 100$ total worldwide). Nevertheless, we were able to add one autism spectrum disorder case and several controls that could not be matched as those described in Table 1. With a final cohort of $n = 18$ controls and $n = 13$ autism spectrum disorder subjects, the decrease in calretinin + density again was highly significant ($P = 0.00002$). We extensively analysed the potential effects of sex, post-mortem interval, fixation time, and other variables on calretinin + density and found no significant interactions (Supplementary material).

Previous work found significantly more calretinin + interneurons rostrally than caudally (rodent) and in the caudate compared to the putamen (primate) (Wu and Parent, 2000). We found a significantly higher density of medium calretinin + neurons in the anterior caudate nucleus (from −22.5 mm to −5.8 mm) compared to the posterior caudate nucleus (from −5 mm to 13.3 mm) of controls (anterior: $183 \pm 28.4$ neurons/cm$^2$, posterior: $72 \pm 13$ neurons/cm$^2$, $P = 0.002$, Mann-Whitney U-test). This anterior–posterior difference was not statistically significant in autism spectrum disorder (anterior: $112 \pm 23$ neurons/cm$^2$, posterior:

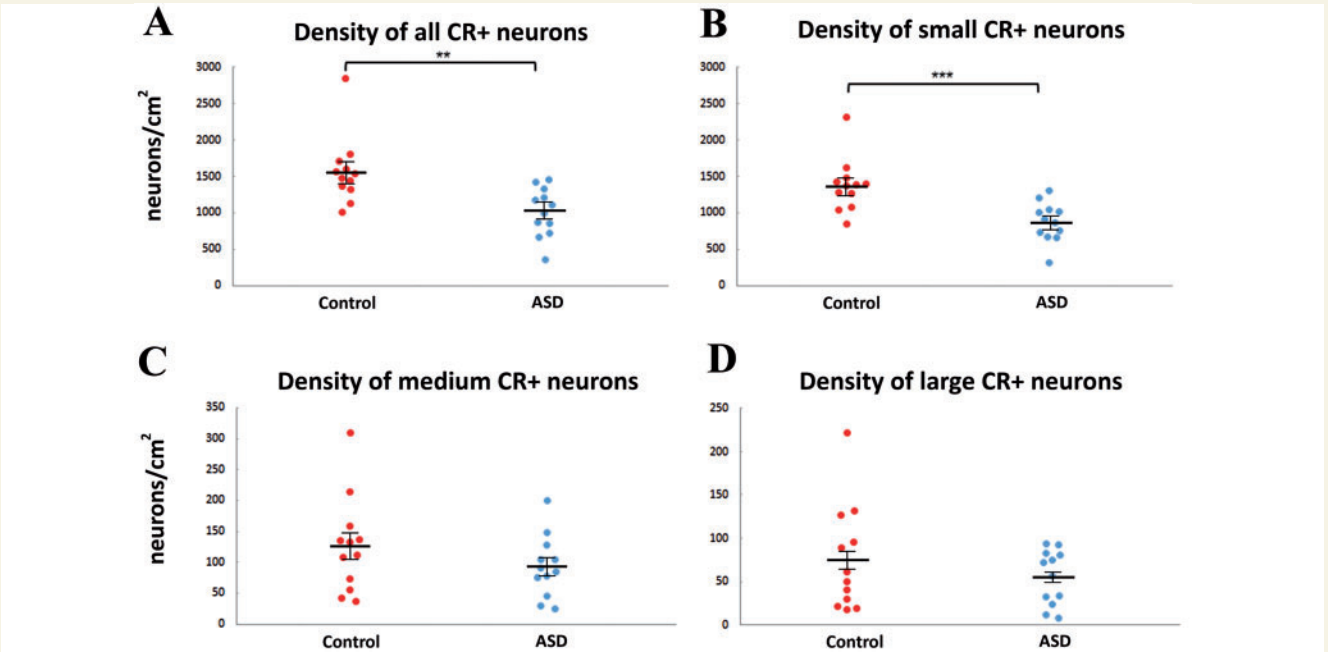


**Figure 2 The density of calretinin + neurons is lower in subjects with autism than in controls.** Graphs showing the number of calretinin + (CR + ) neurons per square centimetre as a total population (**A**) and subdivided into the small (**B**), medium (**C**) and large (**D**) diameter populations. $n = 12$ each controls and patients with autism. $^{**}P < 0.01$, $^{***}P < 0.001$, Mann-Whitney U-test.

77 ± 17 neurons/cm$^2$, $P = 0.310$). Furthermore, there was a significant correlation between the density of medium calretinin + neurons and the position of sampling in controls (r = −0.799, $P = 0.002$) but not in autism spectrum disorder (r = −0.547, $P = 0.066$, Spearman's rank test). The small and large calretinin + neurons were not significantly affected by position of sampling (Supplementary material, univariate ANOVA). Heatmap distributions of calretinin + neurons revealed no conspicuous difference in hot spots of calretinin + neurons in the caudate nucleus in both diagnostic groups (Supplementary Fig. 3). In support of this, cluster analysis in the coronal plane carried out with Matlab did not reveal any calretinin + total, small, medium or large clustering in either diagnostic group tested with multiple algorithms (data not shown).

## Calretinin + density in the caudate nucleus increases with age in controls but not in patients with autism spectrum disorder

We next examined the relationship between the density of calretinin + neurons and age (Supplementary Fig. 4). There was a significant positive correlation between large and medium calretinin + density and age in the caudate nucleus of controls (r = 0.746, $P = 0.005$; r = 0.725; $P = 0.008$, large and medium, respectively). Interestingly, this correlation was not found in autism spectrum disorder (r = 0.481, $P = 0.114$, r = 0.497; $P = 0.100$, large and medium, respectively). We found no correlation between small calretinin + neuron density and age in controls (r = 0.352, $P = 0.262$) or subjects with autism (r = 0.327, $P = 0.300$). Furthermore, we found a 308% increase in the density of large calretinin + caudate nucleus neurons in controls >35 years ($n = 5$) compared to younger individuals ($n = 7$) ($P = 0.018$), but this was not observed in subjects with autism ($P = 0.461$). Medium calretinin + neurons were also more abundant in controls > 35 years (189% increase, $P = 0.048$), but not in subjects with autism ($P = 0.283$).

## Caudate nucleus size was not significantly different between subjects with autism and controls

Ninety-five coronal cross-sectional surface areas (surface area) from 95 different slabs (50 from controls and 45 from autism spectrum disorder) were measured in our cohorts from nine controls and nine patients with autism where multiple regions of the caudate nucleus were available. There was no significant difference in the average surface area between groups (controls: 1.22 ± 0.09 cm$^2$, autism spectrum disorder: 1.19 ± 0.09 cm$^2$ $P = 0.863$). The average position of the sections was similar between controls and subjects with autism (controls:−6.20 ± 1.36 mm, autism spectrum disorder: −5.10 ± 1.60 mm, from the anterior commissure, $P = 0.591$) and they corresponded well with the position of the original slides (controls: −8.06 ± 1.35 mm, autism spectrum disorder: −4.89 ± 2.36 mm).

There was no significant correlation between caudate nucleus surface area and age in either group (Supplementary material, controls: r = 0.492, $P = 0.179$; autism spectrum disorder: r = 0.209, $P = 0.589$) nor significant difference in caudate nucleus surface area between younger (age ⩽ 35) or older (age > 35) in controls ($P = 0.548$) or subjects with autism ($P = 0.905$). ANOVA revealed no statistically significant effects of any of the following variables on caudate nucleus surface area: diagnosis, gender, hemisphere, postmortem interval and time in paraformaldehyde (Supplementary Table 6). These data indicate that there were no significant caudate size differences between controls and subjects with autism spectrum disorder.

## The density of calretinin + neurons in the cerebral cortex

The anterior cingulate cortex was present in a subset of the slides (five controls and five autism spectrum disorder cases) therefore our analysis was extended to this region as well. The dominant calretinin + neuronal type had elongated and bipolar morphology (Supplementary Fig. 5A and B). There were no obvious differences in calretinin + neuron morphology or size between controls and subjects with autism spectrum disorder (Supplementary Fig. 5). We found markedly different densities of calretinin + neurons in distinct layers of the cerebral cortex in both diagnostic groups (Supplementary Fig. 6). The frequency distribution of calretinin + neurons in the human cortex was similar to that observed in macaque (Gabbott, 2016). The density of calretinin + neurons was not statistically different from controls even though the density was 33.3% lower overall in the autism group ($P = 0.151$, Supplementary Fig. 5C). Comparing the layerwise distribution, there was a trend to a lower density of calretinin + neurons in layers 2–6 but a greater density in layer 1 of subjects with autism compared to controls (Supplementary Fig. 6A and C). Statistically significant lower density in autism spectrum disorder was only found in layer 5 (38.5%, $P = 0.032$, Supplementary Fig. 6C). We compared calretinin + neuronal density in the caudate nucleus versus the cingulate cortex but found no statistically significant correlation in control (r = 0.2, $P = 0.747$) or autism spectrum disorder subjects (r = 0.3, $P = 0.624$).

## No evidence for altered corticostriatal circuitry in autism spectrum disorder

We carried out post-mortem tractography on two subjects with autism, a 22-year-old male (Case 07/09) and a 60-year-old female (Case 29/12) (Smith *et al.*, 2004; Behrens

et al., 2007; Miller et al., 2011). Both showed a similar set of white matter tracts connecting the prefrontal cortex with the anterior/middle caudate nucleus (Supplementary Fig. 7 and Supplementary Table 8). These results are consistent with previous studies demonstrating connectivity between the cortex and the caudate nucleus (Robinson et al., 2012; Delmonte et al., 2013).

## Morphology and density of neuropeptide Y + neurons did not significantly differ between controls and subjects with autism

Two types of neuropeptide Y + neurons were distinguished based on their characteristic morphology (Fig. 3). Many had round to oval perikarya usually with one to two primary processes (fusiform neurons). Fewer neuropeptide Y + neurons had obvious pyramidal or multipolar perikarya usually with two to three primary processes (neurogliaform neurons). Both types of cell bodies ranged in diameter from 6 to 40 µm. There were no conspicuous morphological differences in caudate nucleus neuropeptide Y + neurons between the control and autism spectrum disorder groups.

We quantified every neuropeptide Y + neuron present in the caudate nucleus in our sections. Altogether, 4977 neurons in the control group and 4567 neurons in the autism spectrum disorder group were counted. No significant differences were found between the diagnostic groups in the average diameters of the neuropeptide Y + neurons (controls: $14.33 \pm 0.32$ µm, autism spectrum disorder: $14.66 \pm 0.43$ µm, $P = 0.41$). We found a 12.7% lower density in neuropeptide Y + neurons in autism spectrum disorder; however, it was not statistically significant (controls: 423.66 cells/cm$^2$, autism spectrum disorder: 369.66 cells/cm$^2$, $P = 0.143$).

Similar to the lack of effect of diagnosis on the density of neuropeptide Y + neurons ($F = 3.055$, df = 7,16, $P = 0.102$), there were no significant effects of other variables, such as gender, hemisphere, age or antero-posterior position of sampling (Supplementary Table 7). There were also no significant effects of potential confounders on the density of neuropeptide Y + neurons, such as post-mortem interval, fixation time in paraformaldehyde, time in paraffin and processing time (Supplementary Table 7).

## Microglia were not activated in autism spectrum disorder

To determine if the decrease in calretinin + density was associated with increased inflammation, we carried out immunohistochemistry for the microglial marker IBA1 (Ito et al., 1998). Qualitative assessment of IBA1 + microglial morphology in the caudate nucleus by three independent observers did not reveal obvious microglial morphology differences between controls and autism spectrum disorder cases (Fig. 4A and B), using previously established criteria (Goings et al., 2008). Microglia in the caudate nucleus of both controls and subjects with autism had typical resting microglial shape with small cell bodies, fine ramified processes and moderate IBA1 immunohistochemistry (Fig. 4A and B).

Quantitative analysis revealed no statistical difference between controls and autism spectrum disorder in the IBA1 immunopositive area fraction (controls: $3.16\% \pm 0.49\%$, autism spectrum disorder: $3.78\% \pm 0.63\%$, $P = 0.799$, Mann-Whitney U-test, Fig. 4C). The IBA1 stained area fraction (percentage of IBA1-immunopositive area per total area) did not have a significant effect on the density of calretinin + neurons in either subjects with autism or controls ($F = 0.066$, df = 7, 13, $P = 0.803$) (Supplementary Table 4) or on the density of neuropeptide Y + neurons ($F = 1.327$, df = 7, 14, $P = 0.274$) (Supplementary Table 7). Finally, there were no significant interactions between the IBA1 stained area fraction and the density of small, medium or large calretinin + neurons in either diagnostic group (univariate ANOVA, Supplementary Table 5).

# Discussion

We have discovered one of the most striking examples of altered neuronal numbers in the forebrain in autism spectrum disorder; a highly significant decrease in calretinin + neuronal density in the caudate nucleus. Rather than sampling, we counted all calretinin + cells in our material, a total of 30 613 calretinin + neurons. In line with the observations of Petryszyn et al. (2014) we confirmed that there are three populations; small, medium and large calretinin + interneurons in the human caudate nucleus. Furthermore, our data on the proportions of small, medium and large calretinin + neurons in controls correspond well with previous stereological data (Bernacer et al., 2012). Several reports claim that autism spectrum disorder is associated with increased head and brain size and expansion of particular brain subregions (Courchesne et al., 2003). Wegiel et al. (2014a, b) reported increased caudate volume in autism spectrum disorder. If our autism spectrum disorder cases had expanded caudate nucleus, it could have contributed to the decreased calretinin + cell density. However, we carried out careful measurements and found that the cross-sectional surface areas of the caudate nucleus were very similar between controls and patients with autism. Others also found that the caudate volume is not significantly different in autism spectrum disorder compared to controls (McAlonan et al., 2002; Hardan et al., 2003; Herbert et al., 2003; Ecker et al., 2012; Langen et al., 2012; Hua et al., 2013; Lin et al., 2015; Sussman et al., 2015).

There is a remarkable dearth of information about the connectivity, electrophysiological properties and function of calretinin + neurons in the caudate nucleus. However, in the cerebral cortex, bipolar calretinin + neurons

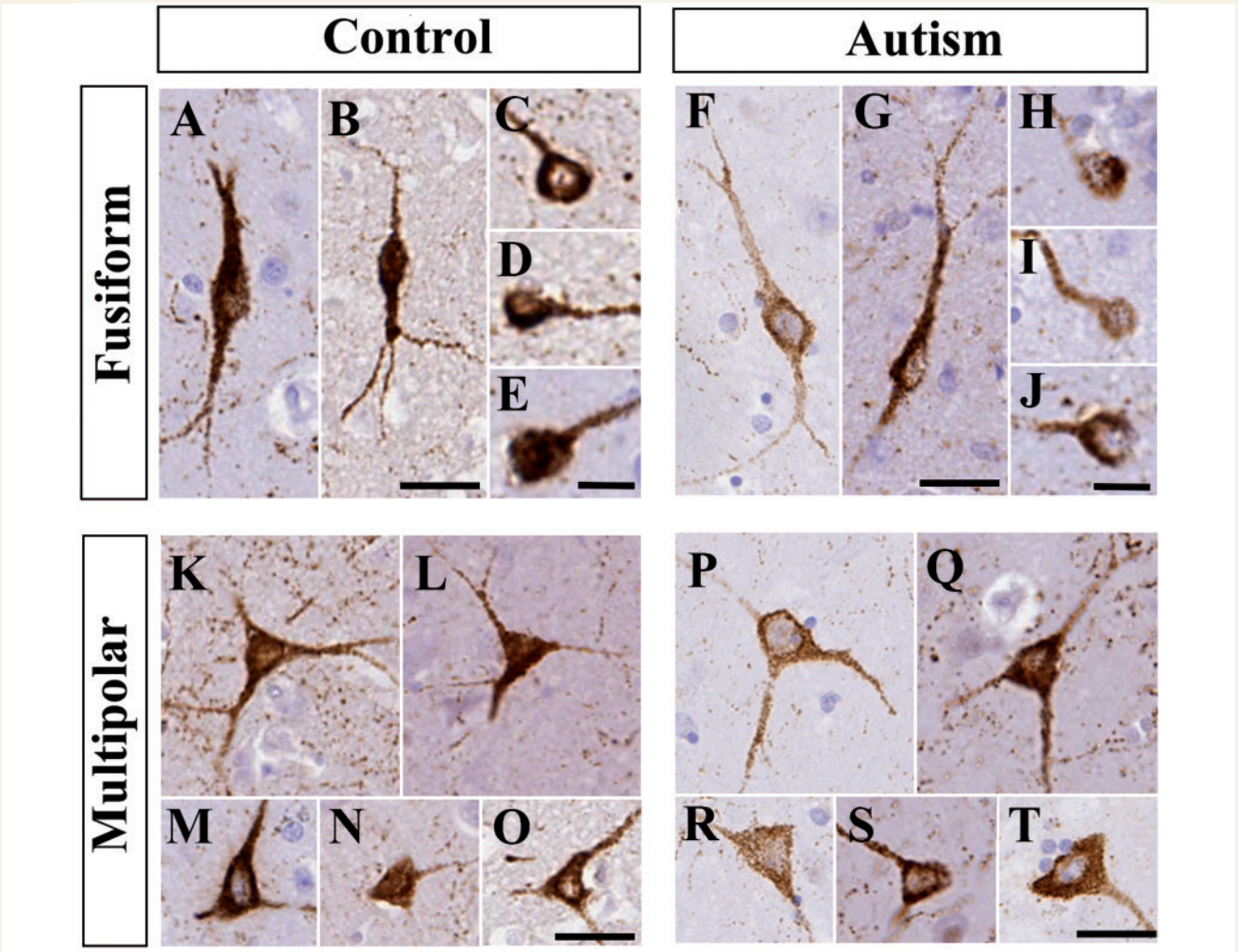


**Figure 3 The morphology of neuropeptide Y + neurons in the caudate nucleus was similar in controls and subjects with autism.** Images were taken from *n* = 5 controls and *n* = 5 patients with autism. (**A–E**) Fusiform neuropeptide Y + neurons in controls. (**F–J**) Fusiform neuropeptide Y + neurons in subjects with autism. (**K–O**) Multipolar neuropeptide Y + neurons in controls. (**P–T**) Multipolar neuropeptide Y + neurons in autism spectrum disorder. Scale bars in **C–E**, **H–J** = 10 μm, otherwise 30 μm.

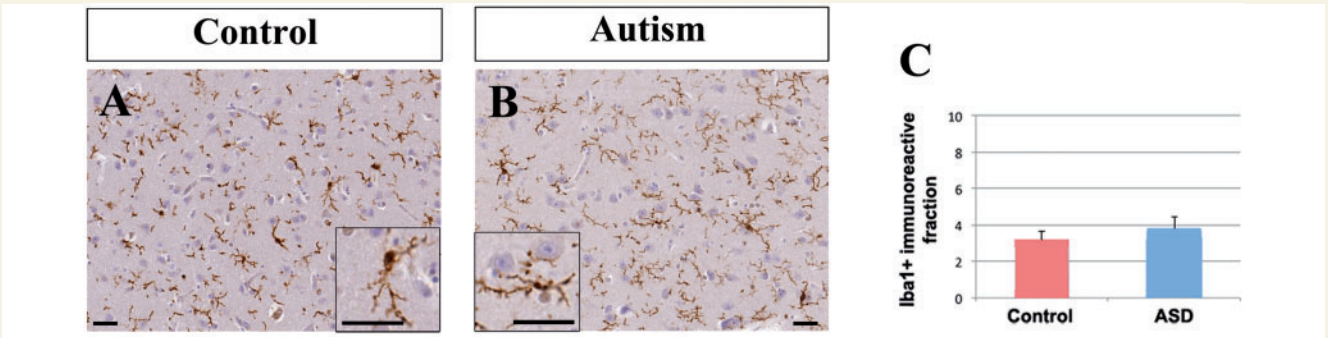


**Figure 4 IBA1 + cells were similar between controls and subjects with autism.** The distribution, intensity of immunostaining and morphology of IBA1 + cells was not appreciably different between controls (**A**) and patients with autism (**B**). Scale bars = 30 μm. (**C**) The surface area occupied by IBA1 + immunoreactivity in the caudate nucleus was not significantly different between controls and subjects with autism spectrum disorder.

preferentially target layer 2/3 multipolar calretinin + neurons and layer 5 pyramidal neurons, whereas multipolar calretinin + neurons maintain theta-oscillations via inhibition of parvalbumin + neurons that innervate layer 2/3 pyramidal neurons (Meskenaite, 1997; Gonchar and Burkhalter, 1999; Caputi *et al.*, 2009). Other important results suggest calretinin is a calcium-modulator limiting hyperexcitation of Purkinje cells (Schiffmann *et al.*, 1999) and maintaining long term potentiation (LTP) in the dentate gyrus (Schurmans *et al.*, 1997). Calretinin + neuronal function in the caudate nucleus may be poorly understood because they account for only 0.5% of neurons in rodents (Rymar *et al.*, 2004). Remarkably, they are estimated to comprise 10% of caudate nucleus neurons in non-human primates (Deng *et al.*, 2010) and humans (Wu and Parent, 2000). However, calretinin + neuron density in the rostral caudate nucleus is comparable across species (Wu and Parent, 2000). Given our results, future studies are warranted to elucidate neuronal inputs to calretinin + neurons in the caudate nucleus and whether they innervate local interneurons or medium spiny neurons. If they primarily regulate local interneurons they may disinhibit medium spiny neurons. If they directly innervate medium spiny neurons they may inhibit the principal cells of the striatum. It will also be important to determine if the large, medium and small calretinin + neurons have different connectivity and thus segregate function.

A major question that arose during our studies was if the decreased density of calretinin + neurons could be generalized to multiple brain areas or if it was specific to the caudate nucleus. Our results revealed a lower density of calretinin + neurons in the anterior cingulate cortex of autism spectrum disorder subjects that was not statistically significant compared to controls. A comparable decrease was found in the CNTNAP2 knockout mouse model of autism spectrum disorder in the somatosensory cortex (Penagarikano *et al.*, 2011). However, in autism the human dorsolateral prefrontal cortex (Brodmann areas 9 and 46) and the ventrolateral prefrontal cortex (Brodmann area 47) did not exhibit decreased densities of calretinin + neurons (Hashemi *et al.*, 2017). It will be important to determine if calretinin + interneurons in other cortical regions may exhibit altered densities in autism spectrum disorders. Based on our results thus far it appears that the caudate nucleus is the site of the greatest decreases in calretinin + cell densities.

It will be important to probe the interrelated functions of dopaminergic neurotransmission and the large calretinin + / cholinergic neurons. Interestingly, 90% of the large calretinin + neurons are cholinergic (Massouh *et al.*, 2008) and cholinergic caudate nucleus interneurons profoundly influence dopaminergic neurotransmission in the caudate nucleus (Threlfell *et al.*, 2012). The density of calretinin + neurons is altered after 6-OHDA and L-DOPA treatment in rat (Mura *et al.*, 2000; Ma *et al.*, 2014), suggesting they are responsive to dopaminergic inputs. Non-human primates have similar calretinin + caudate nucleus neurons to humans (Petryszyn *et al.*, 2014) and primate models of autism spectrum disorder are being developed (Liu *et al.*, 2016), which may also help elucidate the role of calretinin + caudate neurons. Rodent models may also help to reveal calretinin + neuronal function, for example, caudate nucleus function is disturbed in mice with mutations in *Shank3*, a gene associated with autism spectrum disorder (Peca *et al.*, 2011).

An important caveat to these findings is that the relatively late changes in density of medium and large calretinin + neurons in autism spectrum disorder may not contribute to pathophysiology in the first few years of life. It is also possible that these late changes reflect a secondary compensatory mechanism to other events in autism spectrum disorder. For example, calretinin + neuron density or expression could be modulated by seizures, which are a common co-morbidity in autism. Several studies discovered increased calretinin + neuron density in the context of seizures in humans (Blumcke *et al.*, 1999; Kuchukhidze *et al.*, 2015; Wimmer *et al.*, 2015). Interestingly, animal models of neonatal hypoxic brain injury induce the subventricular zone neurogenic niche to generate calretinin + neurons that migrate to the striatum (Yang *et al.*, 2008). These studies suggest that indeed calretinin + neuron numbers can be modulated, but these scenarios increased calretinin + numbers and would not explain the decreased density of calretinin + neurons we observed in this study.

The decreased calretinin + neuron density correlates with expected effects of genetic mutations in autism spectrum disorder (Gene Scoring Module of the SFARI website; https://gene.sfari.org/autdb/GS_Home.do). The *CALB2* gene (encoding calretinin) is a downstream target of the following autism spectrum disorder syndromic genes: *PAX6*, *ARX*, *CTNNBIP1* and *TBR1* (high confidence gene). Mutations in these genes decrease CALB2 (calretinin) expression in animal models and cells (Bedogni *et al.*, 2010; Quille *et al.*, 2011; Ha *et al.*, 2012; Wisniewska, 2013; Huang and Hsueh, 2015); however, calretinin mRNA or protein levels have not been investigated in humans carrying the aforementioned mutations. We do not know the genetic profile of the cases investigated in this study and they were fixed in paraformaldehyde or embedded in paraffin for many years, which hinders molecular investigation.

The caudate nucleus regulates movement, emotion and reward; three modalities that are central in the pathophysiology of autism spectrum disorder. The caudate nucleus has been implicated as a nexus in the pathophysiology of schizophrenia (Simpson *et al.*, 2010), a neuropsychiatric disorder with genetic and behavioural features in common with autism spectrum disorder (Gao and Penzes, 2015; Kastner *et al.*, 2015; Li *et al.*, 2015). The caudate nucleus—especially its rostral part, the pre-commissural head—receives major axonal input from the ventromedial prefrontal cortex, orbitofrontal cortex, dorsolateral prefrontal cortex and anterior cingulate cortex (Haber and Behrens, 2014). These functional cortical inputs to the

caudate nucleus are being actively investigated in autism spectrum disorder and several are impaired (Fatemi *et al.*, 2002; Oblak *et al.*, 2009, 2011; Watanabe *et al.*, 2013; Hashemi *et al.*, 2017) or increased (Delmonte *et al.*, 2013). Interestingly, Delmonte *et al.* (2013) showed within their study that despite increased corticostriate functional connectivity there were no differences between controls and autism spectrum disorder in structural connectivity. Thus far, our pilot work also suggests structural corticostriatal inputs may not be altered; the present results show no obvious deviation from the typically developed architecture. However, considering the small number of subjects with available MRI data, it was not possible to carry out a quantitative diffusion tensor imaging analysis of white matter microstructure (Smith *et al.*, 2004; Behrens et al., 2007; Miller et al., 2011).

The nucleus accumbens is similar in connectivity and neuronal subtypes to the caudate nucleus and they have overlapping functions. Mouse models of repetitive movements show that the nucleus accumbens mediates the effects of the autism-associated gene neuroligin 3 (*NLGN3*) (Rothwell *et al.*, 2014). The globus pallidus, a major target of the caudate nucleus, is reduced in volume compared to the cerebrum in autism spectrum disorder (Estes *et al.*, 2011; Sussman *et al.*, 2015). Thus it will be important to examine not only the cortical inputs to the caudate but also its connectivity of the nucleus accumbens and globus pallidus.

Altered peripheral and central inflammation has been reported in autism spectrum disorder (Vargas *et al.*, 2005; Depino, 2013), and could have contributed to the reduced number of calretinin + neurons. Previously, activated microglia were found in a subset of autism spectrum disorder cases (Vargas *et al.*, 2005; Morgan *et al.*, 2010). However, we found no differences between subjects with autism and controls in the level of IBA1 + immunohistochemistry. The morphology of microglial cells in controls and subjects with autism was also very similar and typical of resting ramified microglia, suggesting lack of inflammation in the caudate nucleus at the time of death. Inflammation may have occurred at earlier time points and it is possible that other indices of inflammation are altered in autism spectrum disorder. If inflammation mediated calretinin + neuron death were prevalent we would have expected to see some damaged or dysmorphic calretinin + cells but the cells generally appeared to be healthy in both groups, with well-defined edges and intact processes.

Our analysis was originally inspired by several findings. First, we discovered that more ependymal cells of the lateral ventricles expressed GFAP in autism spectrum disorder compared to controls (Kotagiri *et al.*, 2014) suggesting neurogenic activation similar to stroke (Carlen *et al.*, 2009; Young *et al.*, 2013). Second, human postnatal neurogenesis may contribute calretinin + and neuropeptide Y + neurons to the caudate nucleus, with a reported 2.7% median turnover rate per year in adulthood (Ernst *et al.*, 2014). We are unsure if the changes we observe are due to reduced neurogenesis but may partially be so. Medium and large calretinin + neuronal numbers significantly increased with age in controls, but not in subjects with autism. The simplest explanation for this is continuous addition of calretinin + neurons to the caudate nucleus via adult neurogenesis in controls but not in subjects with autism. Another explanation may be relatively greater calretinin expression and immunoreactivity in controls compared to subjects with autism, with neuronal density remaining unchanged. This would still be interesting as loss of calretinin inhibits LTP (Schurmans *et al.*, 1997) and changes in its expression could disrupt the inhibitory/excitatory balance in the caudate nucleus. This is a possibility, but we believe it is not likely as the level of expression of calretinin in the caudate appeared to be equivalent in controls and subjects with autism. Unless the decrease in expression occurred before the ages examined, we would have expected to see faint calretinin immunohistochemical detection in at least a subset of autism spectrum disorder neurons. In addition to calretinin and neuropeptide Y expressing interneurons, other populations such as parvalbumin and somatostatin expressing interneurons exist in the caudate nucleus and may have altered densities in subjects with autism. It will be important to determine in future studies if the effect in the caudate is also found in other interneuron populations.

We achieved our goal of determining potential differences in the caudate nucleus between subjects with autism and controls even though autism spectrum disorder is heterogeneous and the cases ranged across ages. Given the heterogeneity of autism spectrum disorder, it was all the more remarkable that we found significant differences and it suggests that the reduction in calretinin + neuron density may occur in multiple subtypes of the disease. We found significant differences, and subsequent studies will determine if autism spectrum disorder subtypes differ in calretinin + density. Interestingly, *Cntnap2*$^{-/-}$ mice have similarities with several core features of autism spectrum disorder and display decreased numbers of GABAergic interneurons in the caudate nucleus and fewer calretinin + interneurons in the cerebral cortex (Penagarikano *et al.*, 2011). Several laboratories have learned how to differentiate caudate interneurons from human induced pluripotential stem cells (Maroof *et al.*, 2013; Nicholas *et al.*, 2013). Thus, future studies using human induced pluripotential stem cells or animal models may help dissect the molecular mechanisms leading to reduced numbers of calretinin + neurons and thus lead to pharmacological interventions.

# Acknowledgments

We acknowledge the Oxford Brain Bank, supported by the Medical Research Council (MRC), Brains for Dementia Research (BDR) and the NIHR Oxford Biomedical Research Centre. Brain donations from some of those

subjects with autism were acquired by the UK Autism Brain Bank which was supported financially by the UK charity 'Autistica'. We thank Ms Carolyn Sloan, Ms Marie Hamard and Mr Connor Scott for their help with sample collection and Ms Ana Xambre Pereira for help with the Nissl stain.

# Funding

This study was supported by a Simons Foundation SFARI grant (249449) and a DANA foundation Grant (to F.G.S.).

# Supplementary material

Supplementary material is available at *Brain* online.

# References

Barinka F, Druga R, Marusic P, Krsek P, Zamecnik J. Calretinin immunoreactivity in focal cortical dysplasias and in non-malformed epileptic cortex. Epilepsy Res 2010; 88: 76–86.

Bedogni F, Hodge RD, Nelson BR, Frederick EA, Shiba N, Daza RA, et al. Autism susceptibility candidate 2 (Auts2) encodes a nuclear protein expressed in developing brain regions implicated in autism neuropathology. Gene Expr Patterns 2010; 10: 9–15.

Behrens TE, Berg HJ, Jbabdi S, Rushworth MF, Woolrich MW. Probabilistic diffusion tractography with multiple fibre orientations: what can we gain? Neuroimage 2007; 34: 144–55.

Bernacer J, Prensa L, Gimenez-Amaya JM. Distribution of GABAergic interneurons and dopaminergic cells in the functional territories of the human striatum. PLoS One 2012; 7: e30504.

Blumcke I, Beck H, Suter B, Hoffmann D, Fodisch HJ, Wolf HK, et al. An increase of hippocampal calretinin-immunoreactive neurons correlates with early febrile seizures in temporal lobe epilepsy. Acta Neuropathol 1999; 97: 31–9.

Caputi A, Rozov A, Blatow M, Monyer H. Two calretinin-positive GABAergic cell types in layer 2/3 of the mouse neocortex provide different forms of inhibition. Cereb Cortex 2009; 19: 1345–59.

Carlen M, Meletis K, Goritz C, Darsalia V, Evergren E, Tanigaki K, et al. Forebrain ependymal cells are notch-dependent and generate neuroblasts and astrocytes after stroke. Nat Neurosci 2009; 12: 259–67.

Chana G, Landau S, Beasley C, Everall IP, Cotter D. Two-dimensional assessment of cytoarchitecture in the anterior cingulate cortex in major depressive disorder, bipolar disorder, and schizophrenia: evidence for decreased neuronal somal size and increased neuronal density. Biol Psychiatry 2003; 53: 1086–98.

Cicchetti F, Prensa L, Wu Y, Parent A. Chemical anatomy of striatal interneurons in normal individuals and in patients with Huntington's disease. Brain Res Brain Res Rev 2000; 34: 80–101.

Coghlan S, Horder J, Inkster B, Mendez MA, Murphy DG, Nutt DJ. GABA system dysfunction in autism and related disorders: from synapse to symptoms. Neurosci Biobehav Rev 2012; 36: 2044–55.

Courchesne E, Carper R, Akshoomoff N. Evidence of brain overgrowth in the first year of life in autism. JAMA 2003; 290: 337–44.

Delmonte S, Gallagher L, O'Hanlon E, McGrath J, Balsters JH. Functional and structural connectivity of frontostriatal circuitry in autism spectrum disorder. Front Hum Neurosci 2013; 7: 430.

Deng YP, Shelby E, Reiner AJ. Immunohistochemical localization of AMPA-type glutamate receptor subunits in the striatum of rhesus monkey. Brain Res 2010; 1344: 104–23.

Depino AM. Peripheral and central inflammation in autism spectrum disorders. Mol Cell Neurosci 2013; 53: 69–76.

Ebrahimi-Fakhari D, Sahin M. Autism and the synapse: emerging mechanisms and mechanism-based therapies. Curr Opin Neurol 2015; 28: 91–102.

Ecker C, Suckling J, Deoni SC, Lombardo MV, Bullmore ET, Baron-Cohen S, et al. Brain anatomy and its relationship to behavior in adults with autism spectrum disorder: a multicenter magnetic resonance imaging study. Arch Gen Psychiatry 2012; 69: 195–209.

Elsabbagh M, Divan G, Koh YJ, Kim YS, Kauchali S, Marcin C, et al. Global prevalence of autism and other pervasive developmental disorders. Autism Res 2012; 5: 160–79.

Ernst A, Alkass K, Bernard S, Salehpour M, Perl S, Tisdale J, et al. Neurogenesis in the striatum of the adult human brain. Cell 2014; 156: 1072–83.

Estes A, Shaw DW, Sparks BF, Friedman S, Giedd JN, Dawson G, et al. Basal ganglia morphometry and repetitive behavior in young children with autism spectrum disorder. Autism Res 2011; 4: 212–20.

Fatemi SH, Halt AR, Stary JM, Kanodia R, Schulz SC, Realmuto GR. Glutamic acid decarboxylase 65 and 67 kDa proteins are reduced in autistic parietal and cerebellar cortices. Biol Psychiatry 2002; 52: 805–10.

Fuccillo MV. Striatal circuits as a common node for autism pathophysiology. Front Neurosci 2016; 10: 27.

Gabbott PL. "Subpial fan cell"—a class of calretinin neuron in layer 1 of adult monkey prefrontal cortex. Front Neuroanat 2016; 10: 28.

Gao R, Penzes P. Common mechanisms of excitatory and inhibitory imbalance in schizophrenia and autism spectrum disorders. Curr Mol Med 2015; 15: 146–67.

Geschwind DH, State MW. Gene hunting in autism spectrum disorder: on the path to precision medicine. Lancet Neurol 2015; 14: 1109–20.

Glerean E, Pan RK, Salmi J, Kujala R, Lahnakoski JM, Roine U, et al. Reorganization of functionally connected brain subnetworks in high-functioning autism. Hum Brain Mapp 2016; 37: 1066–79.

Gogolla N, Leblanc JJ, Quast KB, Sudhof TC, Fagiolini M, Hensch TK. Common circuit defect of excitatory-inhibitory balance in mouse models of autism. J Neurodev Disord 2009; 1: 172–81.

Goings GE, Greisman A, James RE, Abram LK, Begolka WS, Miller SD, et al. Hematopoietic cell activation in the subventricular zone after Theiler's virus infection. J Neuroinflammation 2008; 5: 44–66.

Gonchar Y, Burkhalter A. Three distinct families of GABAergic neurons in rat visual cortex. Cereb Cortex 1997; 7: 347–58.

Gonchar Y, Burkhalter A. Connectivity of GABAergic calretinin-immunoreactive neurons in rat primary visual cortex. Cereb Cortex 1999; 9: 683–96.

Gonchar Y, Wang Q, Burkhalter A. Multiple distinct subtypes of GABAergic neurons in mouse visual cortex identified by triple immunostaining. Front Neuroanat 2007; 1: 3.

Graveland GA, DiFiglia M. The frequency and distribution of medium-sized neurons with indented nuclei in the primate and rodent neostriatum. Brain Res 1985; 327: 307–11.

Ha TJ, Swanson DJ, Kirova R, Yeung J, Choi K, Tong Y, et al. Genome-wide microarray comparison reveals downstream genes of Pax6 in the developing mouse cerebellum. Eur J Neurosci 2012; 36: 2888–98.

Haber SN, Behrens TE. The neural network underlying incentive-based learning: implications for interpreting circuit disruptions in psychiatric disorders. Neuron 2014; 83: 1019–39.

Hardan AY, Kilpatrick M, Keshavan MS, Minshew NJ. Motor performance and anatomic magnetic resonance imaging (MRI) of the basal ganglia in autism. J Child Neurol 2003; 18: 317–24.

Hardan AY, Muddasani S, Vemulapalli M, Keshavan MS, Minshew NJ. An MRI study of increased cortical thickness in autism. Am J Psychiatry 2006; 163: 1290–2.

Hashemi E, Ariza J, Rogers H, Noctor SC, Martinez-Cerdeno V. The number of parvalbumin-expressing interneurons is decreased in the

medial prefrontal cortex in autism. Cereb Cortex 2017; 27: 1931–43.
Herbert MR, Ziegler DA, Deutsch CK, O'Brien LM, Lange N, Bakardjiev A, et al. Dissociations of cerebral cortex, subcortical and cerebral white matter volumes in autistic boys. Brain 2003; 126 (Pt 5): 1182–92.
Hua X, Thompson PM, Leow AD, Madsen SK, Caplan R, Alger JR, et al. Brain growth rate abnormalities visualized in adolescents with autism. Hum Brain Mapp 2013; 34: 425–36.
Huang TN, Hsueh YP. Brain-specific transcriptional regulator T-brain-1 controls brain wiring and neuronal activity in autism spectrum disorders. Front Neurosci 2015; 9: 406.
Ito D, Imai Y, Ohsawa K, Nakajima K, Fukuuchi Y, Kohsaka S. Microglia-specific localisation of a novel calcium binding protein, Iba1. Brain Res Mol Brain Res 1998; 57: 1–9.
Kastner A, Begemann M, Michel TM, Everts S, Stepniak B, Bach C, et al. Autism beyond diagnostic categories: characterization of autistic phenotypes in schizophrenia. BMC Psychiatry 2015; 15: 115.
Kern JK. Purkinje cell vulnerability and autism: a possible etiological connection. Brain Dev 2003; 25: 377–82.
Knapp M, Romeo R, Beecham J. Economic cost of autism in the UK. Autism 2009; 13: 317–36.
Kohls G, Chevallier C, Troiani V, Schultz RT. Social 'wanting' dysfunction in autism: neurobiological underpinnings and treatment implications. J Neurodev Disord 2012; 4: 10.
Kotagiri P, Chance SA, Szele FG, Esiri MM. Subventricular zone cytoarchitecture changes in autism. Dev Neurobiol 2014; 74: 25–41.
Kuchukhidze G, Wieselthaler-Holzl A, Drexel M, Unterberger I, Luef G, Ortler M, et al. Calcium-binding proteins in focal cortical dysplasia. Epilepsia 2015; 56: 1207–16.
Langen M, Leemans A, Johnston P, Ecker C, Daly E, Murphy CM, et al. Fronto-striatal circuitry and inhibitory control in autism: findings from diffusion tensor imaging tractography. Cortex 2012; 48: 183–93.
Li J, Zhao L, You Y, Lu T, Jia M, Yu H, et al. Schizophrenia related variants in CACNA1C also confer risk of autism. PLoS One 2015; 10: e0133247.
Libero LE, Nordahl CW, Li DD, Ferrer E, Rogers SJ, Amaral DG. Persistence of megalencephaly in a subgroup of young boys with autism spectrum disorder. Autism Res 2016; 9: 1169–82.
Lin HY, Ni HC, Lai MC, Tseng WY, Gau SS. Regional brain volume differences between males with and without autism spectrum disorder are highly age-dependent. Mol Autism 2015; 6: 29.
Liu Z, Li X, Zhang JT, Cai YJ, Cheng TL, Cheng C, et al. Autism-like behaviours and germline transmission in transgenic monkeys overexpressing MeCP2. Nature 2016; 530: 98–102.
Ma Y, Zhan M, OuYang L, Li Y, Chen S, Wu J, et al. The effects of unilateral 6-OHDA lesion in medial forebrain bundle on the motor, cognitive dysfunctions and vulnerability of different striatal interneuron types in rats. Behav Brain Res 2014; 266: 37–45.
Mai J, Paxinos G, Voss T. Atlas of the human brain. 3rd edn. New York, NY: Academic Press; 2008.
Maroof AM, Keros S, Tyson JA, Ying SW, Ganat YM, Merkle FT, et al. Directed differentiation and functional maturation of cortical interneurons from human embryonic stem cells. Cell Stem Cell 2013; 12: 559–72.
Massouh M, Wallman MJ, Pourcher E, Parent A. The fate of the large striatal interneurons expressing calretinin in Huntington's disease. Neurosci Res 2008; 62: 216–24.
McAlonan GM, Daly E, Kumari V, Critchley HD, van Amelsvoort T, Suckling J, et al. Brain anatomy and sensorimotor gating in Asperger's syndrome. Brain 2002; 125 (Pt 7): 1594–606.
Meskenaite V. Calretinin-immunoreactive local circuit neurons in area 17 of the cynomolgus monkey, Macaca fascicularis. J Comp Neurol 1997; 379: 113–32.
Miller KL, Stagg CJ, Douaud G, Jbabdi S, Smith SM, Behrens TE, et al. Diffusion imaging of whole, post-mortem human brains on a clinical MRI scanner. Neuroimage 2011; 57: 167–81.
Morgan JT, Chana G, Pardo CA, Achim C, Semendeferi K, Buckwalter J, et al. Microglial activation and increased microglial density observed in the dorsolateral prefrontal cortex in autism. Biol Psychiatry 2010; 68: 368–76.
Mura A, Feldon J, Mintz M. The expression of the calcium binding protein calretinin in the rat striatum: effects of dopamine depletion and L-DOPA treatment. Exp Neurol 2000; 164: 322–32.
Nicholas CR, Chen J, Tang Y, Southwell DG, Chalmers N, Vogt D, et al. Functional maturation of hPSC-derived forebrain interneurons requires an extended timeline and mimics human neural development. Cell Stem Cell 2013; 12: 573–86.
Oblak A, Gibbs TT, Blatt GJ. Decreased GABAA receptors and benzodiazepine binding sites in the anterior cingulate cortex in autism. Autism Res 2009; 2: 205–19.
Oblak AL, Gibbs TT, Blatt GJ. Reduced GABAA receptors and benzodiazepine binding sites in the posterior cingulate cortex and fusiform gyrus in autism. Brain Res 2011; 1380: 218–28.
Peca J, Feliciano C, Ting JT, Wang W, Wells MF, Venkatraman TN, et al. Shank3 mutant mice display autistic-like behaviours and striatal dysfunction. Nature 2011; 472: 437–42.
Penagarikano O, Abrahams BS, Herman EI, Winden KD, Gdalyahu A, Dong H, et al. Absence of CNTNAP2 leads to epilepsy, neuronal migration abnormalities, and core autism-related deficits. Cell 2011; 147: 235–46.
Petryszyn S, Beaulieu JM, Parent A, Parent M. Distribution and morphological characteristics of striatal interneurons expressing calretinin in mice: a comparison with human and nonhuman primates. J Chem Neuroanat 2014; 59–60: 51–61.
Quille ML, Carat S, Quemener-Redon S, Hirchaud E, Baron D, Benech C, et al. High-throughput analysis of promoter occupancy reveals new targets for Arx, a gene mutated in mental retardation and interneuronopathies. PLoS One 2011; 6: e25181.
Robinson JL, Laird AR, Glahn DC, Blangero J, Sanghera MK, Pessoa L, et al. The functional connectivity of the human caudate: an application of meta-analytic connectivity modeling with behavioral filtering. Neuroimage 2012; 60: 117–29.
Rogasch NC, Daskalakis ZJ, Fitzgerald PB. Cortical inhibition, excitation, and connectivity in schizophrenia: a review of insights from transcranial magnetic stimulation. Schizophr Bull 2014; 40: 685–96.
Rothwell PE, Fuccillo MV, Maxeiner S, Hayton SJ, Gokce O, Lim BK, et al. Autism-associated neuroligin-3 mutations commonly impair striatal circuits to boost repetitive behaviors. Cell 2014; 158: 198–212.
Rubenstein JL, Merzenich MM. Model of autism: increased ratio of excitation/inhibition in key neural systems. Genes Brain Behav 2003; 2: 255–67.
Rymar VV, Sasseville R, Luk KC, Sadikot AF. Neurogenesis and stereological morphometry of calretinin-immunoreactive GABAergic interneurons of the neostriatum. J Comp Neurol 2004; 469: 325–39.
Sacco R, Gabriele S, Persico AM. Head circumference and brain size in autism spectrum disorder: a systematic review and meta-analysis. Psychiatry Res 2015; 234: 239–51.
Schiffmann SN, Cheron G, Lohof A, d'Alcantara P, Meyer M, Parmentier M, et al. Impaired motor coordination and Purkinje cell excitability in mice lacking calretinin. Proc Natl Acad Sci USA 1999; 96: 5257–62.
Schurmans S, Schiffmann SN, Gurden H, Lemaire M, Lipp HP, Schwam V, et al. Impaired long-term potentiation induction in dentate gyrus of calretinin-deficient mice. Proc Natl Acad Sci USA 1997; 94: 10415–20.
Simpson EH, Kellendonk C, Kandel E. A possible role for the striatum in the pathogenesis of the cognitive symptoms of schizophrenia. Neuron 2010; 65: 585–96.
Smith E, Thurm A, Greenstein D, Farmer C, Swedo S, Giedd J, et al. Cortical thickness change in autism during early childhood. Hum Brain Mapp 2016; 37: 2616–29.

Smith SM, Jenkinson M, Woolrich MW, Beckmann CF, Behrens TE, Johansen-Berg H, et al. Advances in functional and structural MR image analysis and implementation as FSL. Neuroimage 2004; 23 (Suppl 1): S208–19.

Sussman D, Leung RC, Vogan VM, Lee W, Trelle S, Lin S, et al. The autism puzzle: diffuse but not pervasive neuroanatomical abnormalities in children with ASD. Neuroimage Clin 2015; 8: 170–9.

Threlfell S, Lalic T, Platt NJ, Jennings KA, Deisseroth K, Cragg SJ. Striatal dopamine release is triggered by synchronized activity in cholinergic interneurons. Neuron 2012; 75: 58–64.

Uhlhaas PJ. Dysconnectivity, large-scale networks and neuronal dynamics in schizophrenia. Curr Opin Neurobiol 2013; 23: 283–90.

Vargas DL, Nascimbene C, Krishnan C, Zimmerman AW, Pardo CA. Neuroglial activation and neuroinflammation in the brain of patients with autism. Ann Neurol 2005; 57: 67–81.

Watanabe N, Sakagami M, Haruno M. Reward prediction error signal enhanced by striatum-amygdala interaction explains the acceleration of probabilistic reward learning by emotion. J Neurosci 2013; 33: 4487–93.

Wegiel J, Flory M, Kuchna I, Nowicki K, Ma SY, Imaki H, et al. Brain-region-specific alterations of the trajectories of neuronal volume growth throughout the lifespan in autism. Acta Neuropathol Commun 2014a; 2: 28.

Wegiel J, Flory M, Kuchna I, Nowicki K, Ma SY, Imaki H, et al. Stereological study of the neuronal number and volume of 38 brain subdivisions of subjects diagnosed with autism reveals significant alterations restricted to the striatum, amygdala and cerebellum. Acta Neuropathol Commun 2014b; 2: 141.

Wimmer VC, Li MY, Berkovic SF, Petrou S. Cortical microarchitecture changes in genetic epilepsy. Neurology 2015; 84: 1308–16.

Wisniewska MB. Physiological role of beta-catenin/TCF signaling in neurons of the adult brain. Neurochem Res 2013; 38: 1144–55.

Wu Y, Parent A. Striatal interneurons expressing calretinin, parvalbumin or NADPH-diaphorase: a comparative study in the rat, monkey and human. Brain Res 2000; 863: 182–91.

Yang Z, You Y, Levison SW. Neonatal hypoxic/ischemic brain injury induces production of calretinin-expressing interneurons in the striatum. J Comp Neurol 2008; 511: 19–33.

Young CC, van der Harg JM, Lewis NJ, Brooks KJ, Buchan AM, Szele FG. Ependymal ciliary dysfunction and reactive astrocytosis in a reorganized subventricular zone after stroke. Cereb Cortex 2013; 23: 647–59.